

Absence of Ferromagnetic Instability at the Metal-Insulator Transition in Si-inversion Layers

V. M. Pudalov^{a,b}, M. E. Gershenson^a, and H. Kojima^a

^a Department of Physics and Astronomy, Rutgers University, New Jersey 08854, USA

^b P. N. Lebedev Physics Institute/Lebedev Research Centre in Physics, 119991 Moscow, Russia
(November 21, 2018)

We have measured the Shubnikov-de Haas oscillations in high-mobility Si MOS structures over a wide range of the carrier densities $n \geq 0.77 \times 10^{11} \text{cm}^{-2}$. This range includes the critical density n_c of the metal-insulator transition for two samples studied. The periodicity of oscillations clearly demonstrates that the electron states remain fourfold degenerate down to and at the 2D MIT. Both the effective spin susceptibility χ^* and mass m^* remain finite and show no signatures of divergency at the critical density for both samples studied. To test possible divergency of $\chi^*(n)$ and $m^*(n)$ at even lower densities, we have analyzed the data on $\chi^*(n)$ and $m^*(n)$ in terms of a critical dependence $\chi^*, m^* \propto (n/n_0 - 1)^{-\alpha}$. Our data suggest that χ^* and m^* may diverge at $n_0 \lesssim 0.5 \times 10^{11} \text{cm}^{-2}$ ($r_s \geq 12$), which is significantly smaller than n_c .

71.30.+h, 73.40.Qv

Despite intensive experimental and theoretical efforts (see, e.g., Ref. [1] for a bibliography), the origin of the apparent “metal-insulator transition in two dimensions” (2D MIT) remains to be the subject of ongoing discussion. This phenomenon addresses a fundamental problem of the ground state of strongly correlated and disordered electron systems. In (100) Si inversion layers, the 2D MIT is observed at a sample-dependent critical electron density $n_c \sim 1 \times 10^{11} \text{cm}^{-2}$ [2].

One of the important unsolved problems is a possible magnetic instability [3] in spin or valley systems. The electron-electron interactions drive a 2D system towards magnetic transition; numerical calculations for the critical value of r_s [4] at the instability vary from 13 to 20 [5]. According to these calculations, the ferromagnetic transition is likely to be of first order with a complete rather than a partial (ferrimagnetic) spin polarization. An interesting interpretation [6,7] of the parallel-field magnetoresistance in Si inversion layers suggested a ferromagnetic instability at or very close to n_c [where $n_c \approx (0.8 - 0.85) \times 10^{11} \text{cm}^{-2}$, which corresponds to $r_s \approx 9$]. The idea of magnetic instability and its possible link to the 2D MIT is important and requires a careful examination.

In this Letter, we report on our experimental test of two possible scenarios for the magnetic instability: (i) complete spin and/or valley polarization occurs spontaneously at a sample-dependent critical density of the MIT, and (ii) χ^* diverges at a universal (sample-independent) value of $n = n_0$. To test the first scenario, we measured the Shubnikov-de Haas (SdH) oscillations and determined the degeneracy of the electron system across the 2D MIT in two samples (down to $n = 0.77 \times 10^{11} \text{cm}^{-2}$). We found that the period of oscillations corresponds to the double-degenerate spin and valley states even in the presence of external magnetic field $B \approx 0.5 \text{T}$. This rules out the possibility of a com-

plete spin/valley polarization at the 2D MIT. To test the second scenario, we analyzed independent measurements of $\chi^*(n)$ and $m^*(n)$, and found that each could be described by the same critical dependence $(n/n_0 - 1)^{-\alpha}$, if we impose an upper limit on the density of the instability, $n_0 \lesssim 0.5 \times 10^{11} \text{cm}^{-2}$ ($r_s \geq 12$), and a lower limit on the critical index $\alpha \gtrsim 0.6$. The density n_0 is significantly lower than n_c for the samples studied.

The measurements were performed on two Si-MOS samples: Si6-14 (peak mobility $\mu^{\text{peak}} \simeq 2.2 \text{m}^2/\text{Vs}$) and Si5 ($4.3 \text{m}^2/\text{Vs}$), with the critical density n_c of the apparent MIT $1.0 \times 10^{11} \text{cm}^{-2}$ and $0.77 \times 10^{11} \text{cm}^{-2}$, respectively. The MOS structures are made on a (001)-Si wafer with [100] source-drain orientation; the gate oxide thickness was $\approx 190 \text{nm}$. The density of electrons was controlled by the gate voltage V_g and determined from the period of SdH oscillations. An in-plane field $B_{\parallel} \geq 0.02 \text{T}$ was applied for quenching the superconductivity of the Al contact pads and gate electrode. Details of the experimental technique can be found in Refs. [9,10]

Typical SdH oscillations of the resistivity $\rho_{xx} \equiv \rho$ are shown in Fig. 1 a as a function of B_{\perp} . Due to a high electron mobility, oscillations were detected in fields down to 0.14T . To examine directly the first scenario, we focus on the period of the SdH oscillations, the quantity which is not renormalized by interactions.

For such low densities as presented in Fig. 1, the oscillations $\rho(B_{\perp})$ are “shaped” mostly by the spin energy gaps [8,9,11,12]. Figure 1 b shows that the magnitude of oscillations increases with an in-plane magnetic field B_{\parallel} . This confirms that the ratio of the Zeeman energy $E_Z = g^* \mu_B B_{\perp}$ to the cyclotron energy $\hbar \omega_c$ is within the interval $1/2 < E_Z/\hbar \omega_c < 1$, in good agreement with the measured values of $\chi^*(n)$ [9], which control the calculated energy spectrum (the upper inset to Fig. 1 b). Curve 5 in Fig. 1 a corresponds to the density $n = n_c$ for sample Si6-14. The latter has been determined in the insulating

regime, $\rho \propto \exp(-\Delta/k_B T)$, by extrapolating the density dependence of the activation energy $\Delta(n)$ to zero [13] (see the inset to Fig. 1 b).

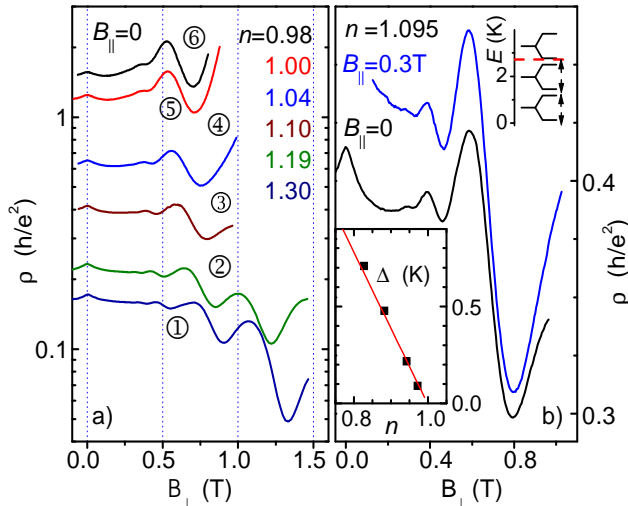


FIG. 1. a) SdH oscillations for the sample Si6-14 at six densities near n_c , $T = 0.2$ K. Curves 3 – 6 are terminated at the onset of a large insulating peak in ρ [14]. b) Enhancement of oscillations with B_{\parallel} . The upper inset shows the energy spectrum for $B_{\perp} = 0.5$ T, $n = 1.0 \times 10^{11} \text{ cm}^{-2}$, $g^*m^*/2m_b = 4.35$, $m^* = 0.5m_e$ [9]. Vertical arrows depict spin polarization and the direction of the corresponding level shift with B_{\parallel} . The lower inset illustrates determination of the critical density for Si6-14. Densities are given in units of 10^{11} cm^{-2} .

In order to emphasize the low-field region, and to clearly illustrate the SdH periodicity, we present the experimental data normalized by the amplitude of the first SdH harmonic $A_1(B_{\perp})$ [15,9]. In evaluating A_1 , we used the values of $\chi^*(n) \propto g^*m^*$ and $m^*(n)$ measured in Ref. [9]; the Dingle temperature was adjusted to match damping of the measured oscillations. Figure 2 shows oscillations of the resistivity $\delta\rho/\rho_0 A_1$ as a function of the Landau level filling, $\nu = nh/eB_{\perp}$. The $\delta\rho(\nu)/\rho_0 A_1$ data (dots) in Figs. 2 a–c correspond to the $\rho(B_{\perp})$ data 1, 5 and 6 in Fig. 1 a. It is important to limit the field range $B_{\perp} \leq 1T$ in the analysis of the SdH oscillations in order to diminish the magnetic-field-induced spin polarization and reentrant quantum Hall effect-to-insulator transitions [14]. The former limitation was violated at $\nu < 5$: doubling of the period for $\nu = 4$ in Fig. 2 a illustrates lifting the spin degeneracy by the perpendicular field $B_{\perp} \sim 1.3T$. The latter limitation was violated for $\nu < 10$ in Figs. 2 b–e and may account for the large oscillation amplitude.

For all the densities studied, including $n = n_c$ (Figs. 2 be), the low-field oscillations $\delta\rho/\rho_0$ have the period $\Delta\nu = 4$ that corresponds to a double-degenerate (*i.e.* unpolarized) spin and valley system. The minima of $\delta\rho$ in Figs. 2 are located at $\nu = 6, 10, 14, 18$, in contrast to

$\nu = 4, 8, 12, 16$, as observed for higher densities. This is in agreement with earlier results [11,12,14] and with the measured χ^* values [9]. The sign of oscillations changes due to the Zeeman factor $\cos(\pi E_Z/\hbar\omega_c)$, when E_Z exceeds $\hbar\omega_c/2$ (at $r_s > 6.3$) [9,15].

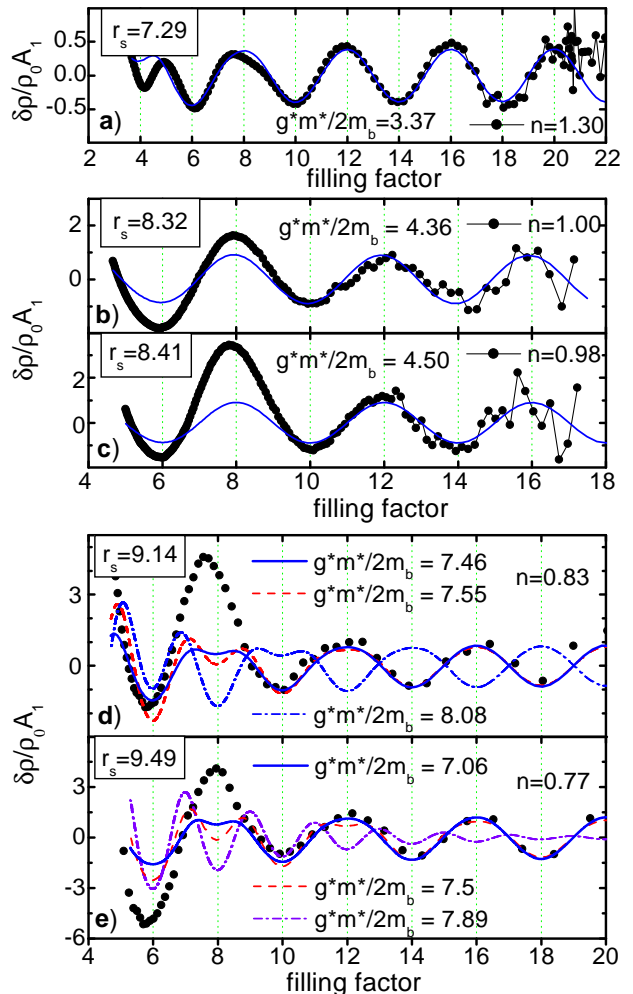


FIG. 2. Oscillatory component of the resistivity measured for samples Si6-14 (panels a–c) and Si5 (panels d, e). The data are shown as dots, the fits as lines [9]; both are normalized by $A_1(B_{\perp})$. The temperature is 0.2 K for traces (a–c) and 0.03 K for traces d and e. The values of n (in units of 10^{11} cm^{-2}), r_s , and g^*m^* are shown in each panel.

From these data, we can estimate the spontaneous spin polarization P_0 near n_c . The total spin polarization of the interacting 2D electron system is:

$$P \equiv \frac{n_{\uparrow} - n_{\downarrow}}{n} = P_Z + P_0 = \frac{\chi^* B_{\perp}}{2\mu_B n} + P_0. \quad (1)$$

Figures 2 c and 2 e show that the complete spin (or valley) polarization does not occur at least down to $\nu = 6$ ($P_Z \approx 0.3$), for both $B_{\parallel} = 0$ and $B_{\parallel} = 0.3T$ (Fig. 1b); thus, the spontaneous component $P_0 < 1 - 0.3 = 0.7$. We

can impose even more restrictive upper limit on the spontaneous spin polarization across the 2D MIT, $P_0 \lesssim 0.18$, by noting that no nodes of beating are seen in SdH oscillations in Figs. 2c, 2e over the interval of $\nu = 5 - 20$. For example, a larger value of $P_0 = 0.19$ would induce a beating node in the SdH oscillations at $\nu = 15$. For even lower densities, the period of the ρ oscillations [11,14] demonstrates that both the spin and valley states remain double-degenerate across the 2D MIT. These *direct* data provide very strong evidence against a complete spontaneous spin/valley polarization at the sample-dependent critical density for $n \geq 0.77 \times 10^{11} \text{cm}^{-2}$.

Below, we explore the second scenario, a divergence of χ^* and m^* at a sample-independent density n_0 . Indeed, it has been found in recent measurements [8,9] that both quantities increase with decreasing carrier concentration and are sample-independent (χ^* - to within $\pm 2\%$, and m^* - $\pm 4\%$). We examine our data on $\chi^*(n)$ and $m^*(n)$ [9,16] for sample Si6-14 for possible critical density dependence in the form $(n/n_0 - 1)^{-\alpha}$. For a given n_0 , the exponents α_χ and α_m have been obtained from fitting $\chi^*(n)$ and $m^*(n)$. An example with $n_0 = 0.53 \times 10^{11} \text{cm}^{-2}$ and $\alpha = 0.63$ is shown in Figs. 3a, b. The exponents α_χ and α_m versus n_0 (hash marks indicate the error bars) are shown in the inset in Fig. 3a. The standard deviation of $\alpha(n_0)$ has such a shallow minimum that the optimal n_0 value could not be determined reliably; the large uncertainty was mainly caused by unknown critical range of densities. Similar uncertain situation was encountered in the critical analysis of the m^* data for sample Si6-14 (see Figs. 3b and 3c).

We now include into consideration the data for sample Si5 which has substantially lower n_c . Three additional $m^*(n)$ points from Si5 are shown as diamonds in Fig. 3c. We find that the critical dependence cannot fit the data when n_0 is taken greater than $0.65 \times 10^{11} \text{cm}^{-2}$; this value sets the upper limit for possible n_0 . Although only the $m^*(n)$ data were available for Si5, $\chi^*(n)$ can be estimated independently from the lineshape and phase of the SdH oscillations. The SdH pattern is very sensitive to the ratio $E_Z/\hbar\omega_c$: when this ratio becomes greater than $3/2$ ($g^*m^* \geq 7.89$) or smaller than $1/2$ ($g^*m^* \leq 2.63$), the phase of oscillations changes by π . Theoretical curves in Figs. 2d and 2e show that, even before the phase reverses for all oscillations, the highest-field oscillation ($\nu = 6$) splits starting from $g^*m^* \approx 7$. The absence of such behavior in the measured $\delta\rho(B_\perp)$ traces enables us to obtain, correspondingly, the upper and lower estimates for g^*m^* at six densities in the range from $n = 0.768$ to $0.884 \times 10^{11} \text{cm}^{-2}$. Three of these estimates are shown by vertical bars in Fig. 3a (three others, located between the shown bars, are omitted for clarity).

Small values of $n_0 \ll n_c$ can be certainly accommodated by the critical dependence; however, we searched for the upper limit on n_0 , in order to determine how close n_0 could be to n_c . For this reason, we have used the *up-*

per limits for χ^* (the top of bars in Fig. 3a) when we plotted the critical dependence in Fig. 3a. The $\chi^*(n)$ data for both Si5 and Si6-14 obey a common critical dependence only if we choose $n_0 \lesssim 0.53 \times 10^{11} \text{cm}^{-2}$. This choice of n_0 also provides the lower limit for the critical index $\alpha_\chi \geq 0.63$. This procedure defines the range of densities where the critical behavior holds: e.g., for $n_0 = 0.53 \times 10^{11} \text{cm}^{-2}$, this range corresponds to $n < 1.5 \times 10^{11} \text{cm}^{-2}$. A similar but less restrictive conclusion follows from the critical analysis for m^* (Figs. 3b,c): $n_0 \lesssim 0.65 \times 10^{11} \text{cm}^{-2}$ and $\alpha_m \geq 0.4$. It is important to note that the upper limit on n_0 is a factor of 1.5-2 lower than the critical density n_c for the samples studied.

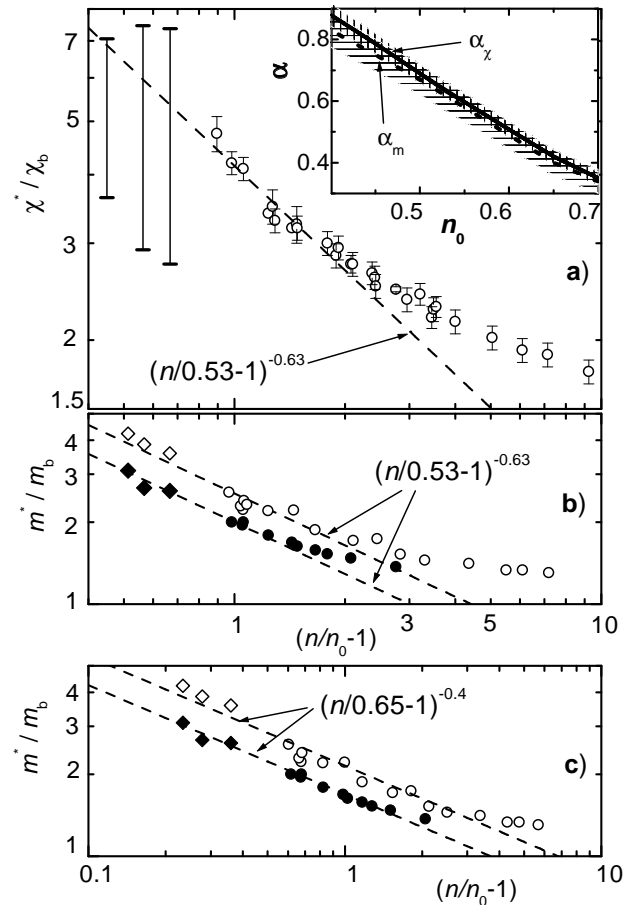


FIG. 3. Log-log plots of (a) the spin susceptibility χ^*/χ_b and (b,c) the mass m^*/m_b vs $(n/n_0 - 1)$: dots for sample Si6-14, diamonds and bars for Si5. The $m^*(n)$ data are plotted for two values of $n_0 = 0.53$ and $0.65 \times 10^{11} \text{cm}^{-2}$. On panels (a): the vertical bars extend from the upper to lower limits for χ^* , as discussed in the text. On panels (b,c): open and closed symbols depict the upper and lower estimate for m^* , obtained from the T -dependence of SdH amplitude [9,16]. The dashed lines show the critical behavior $\chi^*, m^* \propto (n/n_0 - 1)^{-\alpha}$. The inset shows the critical indices α_χ and α_m vs n_0 .

For a given n_0 value, the estimated critical indices α_χ

and α_m are close to each other (see the inset to Fig. 3a). This might be expected: there is no experimental indication for a critical behavior of $g^*(n)$ [9,18], therefore $\chi^* \propto g^*m^*$ and m^* should exhibit the same n -dependence (a critical behavior or otherwise).

The conclusion on the absence of the magnetic instability at $n \approx n_c$, which we have drawn from our analysis, differs from the one suggested in Refs. [6,7]. There might be several reasons for this disagreement. Firstly, we believe that the magnetoresistance data for in-plane fields, analyzed in Refs. [6,7], might be indirectly related to the spin susceptibility of *mobile* electrons. Secondly, measurements in Refs. [6,7] were taken in *strong* in-plane fields. The strong fields drive a 2D system into the hopping regime [17]; the characteristic values of B_{\parallel} go to zero as n approaches n_c [19]. Moreover, even moderate fields $B_{\parallel} < E_F/g^*\mu_B$ induce non-linearity of magnetization, i.e. the $\chi^*(B)$ -dependence [9,20]. In contrast, our *direct* measurements of χ^* have been performed in the *low-field* linear regime.

To summarize, we measured Shubnikov-de Haas oscillations in weak perpendicular fields over a wide density range $n \geq 0.77 \times 10^{11} \text{cm}^{-2}$, which includes the sample-specific critical densities n_c of the 2D MIT for two different samples. It has been found that the period of oscillations corresponds to the fourfold degeneracy of spin/valley systems on both sides of the 2D MIT. Our results demonstrate that the apparent 2D MIT is not accompanied by a spontaneous complete polarization of spins or valleys at zero field. Moreover, the experimental data allow us to put an upper limit $P_0 < 0.18$ on the value of a possible spontaneous polarization at the transition. We also explored a possibility of critical behavior of the renormalized spin susceptibility and the effective mass at a sample-independent density n_0 . We found that the divergence of both χ^* and m^* is unlikely for $n_0 > 0.65 \times 10^{11} \text{cm}^{-2}$. However, it may occur at lower densities (significantly less than n_c): e.g. for χ^* – at $n_0 \lesssim 0.5 \times 10^{11} \text{cm}^{-2}$ and $\alpha \gtrsim 0.6$.

Authors are grateful to E. Abrahams, B. L. Altshuler, and D. L. Maslov for discussions. The work was supported by the NSF, ARO MURI, NWO, NATO, RFBR, INTAS, and the Russian programs “Physics of Nanostructures”, “Quantum and Non-linear Processes”, “Quantum computing and telecommunications”, “Integration of High Education and Academic Research”, and “The State Support of Leading Scientific Schools”.

-
- [1] E. Abrahams, S. V. Kravchenko, and M. P. Sarachik, Rev. Mod. Phys. **73**, 251 (2001).
 - [2] V. M. Pudalov, G. Brunthaler, A. Prinz, G. Bauer, JETP Lett. **68**, 442 (1998). cond-mat/9801077.
 - [3] A. M. Finkelstein, Sov. Sci. Rev. A **14**, 3 (1990).
 - [4] The parameter $r_s = 2.63 \times (10^{12} \text{cm}^{-2}/n)^{1/2}$ which characterizes the electron-electron interactions, is the ratio of the Coulomb interaction energy E_{ee} to the Fermi energy E_F . The bare values of the Fermi energy E_F , the effective mass $m_b = 0.19$, and the dielectric constant $\kappa = 7.8$ at the Si-SiO₂ interface are used in its definition.
 - [5] For reviews, see: G. Senatore, S. Moroni, D. Varzано, Sol. St. Commun. **119**, 333 (2001). A. Isihara and L. C. Ioriatti, Jr., Phys. Rev. B **25**, 5534 (1982).
 - [6] A. A. Shashkin, S. V. Kravchenko, V. T. Dolgopoloв, and T. M. Klapwijk, Phys. Rev. Lett. **87**, 086801 (2001).
 - [7] S. A. Vitkalov, H. Zheng, K. M. Mertez, M. P. Sarachik, and T. M. Klapwijk, Phys. Rev. Lett. **87**, 086401 (2001).
 - [8] T. Okamoto, K. Hosoya, S. Kawaji, and A. Yagi, Phys. Rev. Lett. **82**, 3875 (1999).
 - [9] V. M. Pudalov, M. E. Gershenson, H. Kojima, N. Butch, E. M. Dizhur, G. Brunthaler, A. Prinz, and G. Bauer, Phys. Rev. Lett. **88**, 196404 (2002).
 - [10] M. E. Gershenson, V. M. Pudalov, H. Kojima, N. Butch, E. M. Dizhur, G. Brunthaler, A. Prinz, and G. Bauer, Physica E **12**, 585 (2002).
 - [11] V. M. Pudalov, M. D’Iorio, J. W. Campbell, JETP Lett., **57**, 608 (1993). Surf. Sci. **305**, 107 (1994).
 - [12] S. V. Kravchenko, A. A. Shashkin, D. A. Bloore, T. M. Klapwijk, Sol. State Commun. **116**, 495 (2000).
 - [13] V. M. Pudalov, M. D’Iorio, S. V. Kravchenko, J. W. Campbell, Phys. Rev. Lett. **70**, 1866 (1993).
 - [14] M. D’Iorio, V. M. Pudalov, and S. G. Semenchinsky, Phys. Lett A, **150**, 422 (1990). Phys. Rev. B **46**, 15992 (1992).
 - [15] I. M. Lifshitz and A. M. Kosevich, Zh. Eks. Teor. Fiz. **29**, 730 (1955). A. Isihara, L. Smrčka, J. Phys. C: Solid State Phys. **19**, 6777 (1986).
 - [16] The two values for the effective mass (open and closed symbols) are its upper and lower border [9] and originate from lacking of adequate theory for the temperature dependence of T_D and m^* under conditions of $k_F l \sim 1$.
 - [17] A. A. Shashkin, S. V. Kravchenko, and T. M. Klapwijk, Phys. Rev. Lett. **87**, 266402 (2001).
 - [18] A. A. Shashkin, S. V. Kravchenko, V. T. Dolgopoloв, and T. M. Klapwijk, cond-mat/0111478.
 - [19] V. M. Pudalov, G. Brunthaler, A. Prinz, and G. Bauer, cond-mat/0103087.
 - [20] V. M. Pudalov, M. E. Gershenson, H. Kojima, to be published elsewhere.